

Technical Tips and Imaging in Aortoiliac Intervention

Considerations in selecting noninvasive imaging modalities for use in treating peripheral arterial disease.

BY JOSÉ M. WILEY, MD; PRAKASH KRISHNAN, MD; ELIAS SANIDAS, MD;
JASON C. KOVACIC, MD, PhD; AND GEORGE DANGAS, MD, PhD

Peripheral arterial disease (PAD) is a leading cause of cardiovascular death, amputations, and disability in the industrialized world. The age-adjusted prevalence of PAD is approximately 12%.¹ In the absence of myocardial infarction or stroke, patients with PAD have a similar risk of death from cardiovascular causes as patients with coronary or cerebrovascular disease.² In PAD patients, the rate of death from all causes is elevated, even in those without symptoms. The severity of PAD is closely related to the risk of myocardial infarction, stroke, and death from vascular causes.¹ Patients with critical limb ischemia

(resting pain, ischemic ulcers, or gangrene) have an annual mortality rate of 25%.³

The role of imaging modalities in the management of vascular disease is crucial, with conventional digital subtraction angiography (DSA) considered the gold standard tool for the diagnostic assessment and endovascular treatment of PAD (Figure 1). However, even though DSA has previously been extensively used in this regard, it appears to have certain shortcomings. In recent years, it has been challenged by the rapid development of noninvasive imaging methods such as computed tomographic angiography (CTA), magnetic

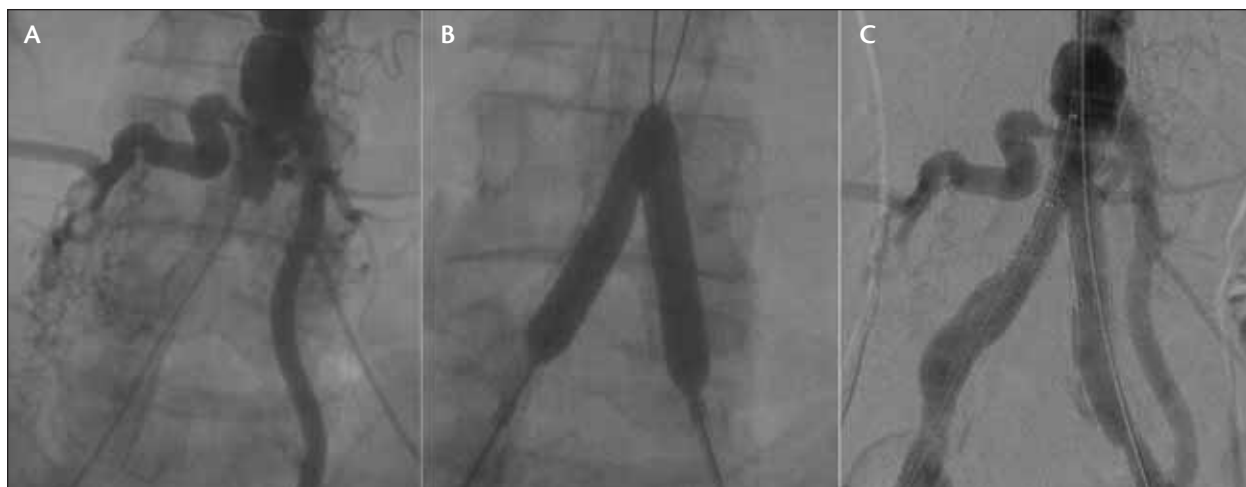


Figure 1. DSA imaging during aortoiliac endovascular intervention for infrarenal aortic occlusion. Distal aortic occlusion with prominent inferior mesenteric artery arising immediately proximal to aortic stump (A). Kissing-balloon dilation of aortoiliac bifurcation following successful recanalization with a 0.035-inch straight, stiff guidewire and with catheter support (B). Final result after endovascular intervention using bilateral balloon-expandable stents (C).

resonance angiography (MRA), intravascular ultrasound (IVUS), and duplex ultrasonography.

CTA

Some studies have reported the superiority of CTA over conventional angiography in the diagnosis of vascular disease.⁴ However, other reports on the diagnostic performance of CTA have provided mixed results.⁵ One limitation of single-slice CTA is the inability to cover the entire length of the abdominal aorta and its branches to the lower legs. The tradeoff between scan volume and spatial resolution along the z-axis of a single-slice CT scan represents a major limitation in the imaging of the aortoiliac arteries with a single contrast injection, because the resolution is not of the same intensity (isotropic) when long vessel segments are covered. This has been resolved with the introduction of MSCTA scanning, which allows imaging of long vascular segments with a single breath hold and thinner slice sections (Figures 2 and 3). CTA can be performed more efficiently with MSCTA because of faster scanning speeds and higher spatial and temporal resolution with a reduced dose of contrast medium.⁵ MSCTA has two major advantages compared to DSA in the detection of PAD. First, eccentric lesions can be precisely evaluated with the use of cross-sectional multiplanar reformatted CTA, which requires only a single-bolus injection. In comparison, multiple views including anteroposterior, oblique, and lateral are required during DSA imaging. Second, MSCTA allows visualization of segments immediately distal to an occlusion that are not opacified by DSA. This can be explained by the fact that the peripheral administration of contrast agent in MSCTA allows for better opacification of the collateral circulation, which in turn allows better opacification of arterial segments distal to the occlusion site. Therefore, arterial occlusions are more frequently diagnosed with CTA than DSA.⁵

One major disadvantage of MSCTA for aortoiliac and lower extremity angiography is the potential for excessive radiation exposure. Further studies are warranted to define the extent and risks of radiation exposure associated with 16- or 64-slice (or even higher-slice) CTA before it may be recommended as an alternative to DSA in the assessment of aortoiliac and lower extremity PAD. Another important drawback of MSCTA is the

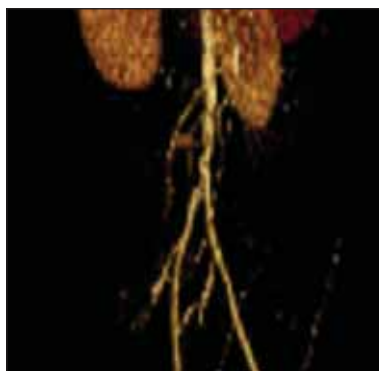


Figure 2. Three-dimensional reconstructed multislice CTA (MSCTA) of distal aortic segment (as also shown in Figure 3). There is no evidence of aneurysmal disease in relation to the ulcerated lesion.

suboptimal imaging of calcified vessels. Ota et al⁶ reported a series of 27 cases of MSCTA utilizing a stratification system based on the severity of arterial calcification. The investigators reported a decreased diagnostic accuracy of MSCTA in vessels with increased calcification. This diagnostic inaccuracy may enhance the potential for overestimation of the severity of luminal stenoses.⁷ The diagnostic accuracy of MSCTA is difficult to ascertain because the ideal gold standard of reference with which to compare a new modality may differ depending on the extent and pattern of the disease.⁸ Sun⁵ reported on the diagnostic value of MSCTA in the diagnosis of PAD

compared with DSA. The pooled sensitivity, specificity, and accuracy rates were 92%, 91%, and 91%, respectively, at all arterial levels; 92%, 94%, and 93% at the aortoiliac arteries; 96%, 85%, and 92% at the femoropopliteal arteries; and 91%, 85%, and 87% at the infrapopliteal arteries.⁵ The lower sensitivity of MSCTA for the detection of aortoiliac versus femoropopliteal disease may be due to the fact that the aortoiliac arteries are more tortuous than those in the lower limb. The presence of high-grade calcification in the aortoiliac region may also explain this difference.⁵ Despite these concerns, with the increasing clinical use of 64-slice CT scanners, MSCTA may be a convenient alternative to DSA in the diagnosis of PAD.

MRA

MRA compares the difference in T1 relaxation times of blood and the surrounding tissues following a rapid bolus infusion of a paramagnetic contrast agent. These gadolinium-based agents exert a T1 shortening effect, generating a high intravascular signal-to-noise ratio that is generally unaffected by inflow. Contrast-enhanced MRA has improved spatial resolution compared to previous MR modalities such as time-of-flight and phase contrast. Contrast-enhanced MRA images represent a record of the vessel lumen, and the timing of scan acquisition is crucial to ensure high-quality images and avoid venous contamination. Hence, bolus-tracking techniques have been used to detect the arrival of contrast. However, contrast-enhanced MRA is limited by the largest available field of view being ≤ 50 cm and the presence of venous signal, which increases with time after contrast injection.⁹ The field-of-view limitation has



Figure 3. DSA imaging during aortoiliac endovascular intervention of distal aortoiliac ulcerated lesion (as shown in Figure 2). Distal aortoiliac lesion (A). Aortoiliac lesion immediately following kissing-balloon dilation (B). Final result after endovascular intervention using bilateral self-expanding stents (kissing-stent technique) (C). Additional extension was required with a proximal right common iliac artery stent due to the length of the iliac stenosis.

been resolved with the use of a stepping-table technique in association with a single contrast injection.¹⁰ Contrast-enhanced MRA has been shown to correlate with DSA in the detection and grading of iliac artery stenoses.¹¹ When intra-arterial pressure measurements are used as a reference, comparable results have been achieved between contrast-enhanced MRA and DSA in assessing iliac artery disease.¹² The three-dimensional quality of MRA, coupled with an arbitrary choice of projections and multiplane reconstructions, offers an additional potential advantage over DSA in assessment of iliac lesions. Contrast-enhanced MRA has thus played a major role in the evaluation of severe stenoses or the occlusion of the aorta and aortoiliac vessels.

A meta-analysis of gadolinium-enhanced MRA in patients with aortoiliac disease reported a pooled sensitivity and specificity of 97.5% and 96.2%, respectively.¹³ However, as a major limitation, MRA in patients with metallic stents is an unsolved challenge. Stents cause magnetic field inhomogeneities, which lead to image distortion and regional loss due to intravoxel dephasing.¹⁴ Band-like artifacts as well as false luminal narrowing are well-described phenomena. Although nitinol stents exhibit less artifacts than steel stents, the delineation of in-stent restenosis remains problematic.¹⁵ Therefore, the inferior ability of MRA to assess in-stent restenosis must be considered when choosing an optimal imaging strategy in patients with endovascular stents.

The concept of interventional MR imaging (MRI) is appealing. A prerequisite for MRI-assisted endovascular

intervention is visualization of catheters and guidewires. There are two methods to visualize hardware: a passive and an active approach. Passive imaging visualizes instruments in a similar fashion as fluoroscopy. Treating the surface of the catheters with gadolinium ions¹⁶ or enhancing the inherent signal void of instruments has offered promising results.¹⁷ Active imaging techniques incorporate radiofrequency microcoils that are embedded into the catheters and guidewires. Thus, the possibility of MRI-assisted endovascular intervention is closer than ever. However, potentially due to inferior spatial resolution, clinical pilot studies have failed to demonstrate any clear advantage of MRI over conventional fluoroscopic intervention.¹⁸

IVUS

IVUS has the ability to overcome several pitfalls of DSA. Fluoroscopic angiography and DSA suffer from the limitation of having only a very limited capacity to define the morphology of an occlusive lesion or the structure of the vessel wall. It is a luminogram that is frequently inaccurate in defining the cross-sectional area and diameter of diseased vessels. Furthermore, angiography has been shown to underestimate residual stenosis in 50% to 80% of treated lesions, particularly those that are eccentric. By comparison, IVUS offers an increased spatial resolution capacity and is able to define vessel and lesion-level detail. IVUS can image vessels in a cross-sectional plane and provide information regarding the morphology of the lesion and the vessel wall, precise cross-sectional measurements, and the location of

important branch vessels. It also provides spatial relationships between a deployed stent and the vessel wall, including the adequacy of stent apposition. Incomplete stent apposition is a known cause of subsequent restenosis and vessel occlusion, and among other applications, IVUS has evolved a niche role in assessing the proper deployment of stents at the conclusion of an endovascular intervention.

DUPLEX ULTRASOUND

Duplex ultrasound is a technical approach that combines high availability with moderate cost. However, it is highly operator-dependent. The examination of the aortoiliac vessels is technically challenging in obese patients or in those with excessive bowel gas or calcified arteries. Pooled sensitivity and specificity are 87.6% and 94.7%, respectively, for the detection of lower limb PAD using color-guided duplex ultrasonography.¹³

CASE REPORT

This case involved an 80-year-old woman with chronic renal insufficiency and significant comorbidities, including refractory hypertension, cervical spinal cord compression (awaiting surgery), coronary artery disease recently treated with bare-metal stent implantation in the left anterior descending coronary artery, and peripheral vascular disease manifesting as severe bilateral claudication (right greater than left). The patient was taking 81 mg of aspirin as well as 75 mg of clopidogrel daily for 1 month after the coronary stent implantation.

At the time of the coronary procedure, severe diffuse aortic atherosclerosis was fluoroscopically documented (Figure 4). The extent of the infrarenal aortic disease was classified as category 3 according to the American Heart Association Task Force on Peripheral Angioplasty.¹⁹

In preparation for the endovascular procedure, a CT scan of the abdominal aorta and iliac arteries was performed on an outpatient basis, which verified the absence of an aortic aneurysm and allowed for precise measurement of aortic lumen dimensions at the proximal and distal reference sites, as well as at the target lesion, and also of the distance between the target

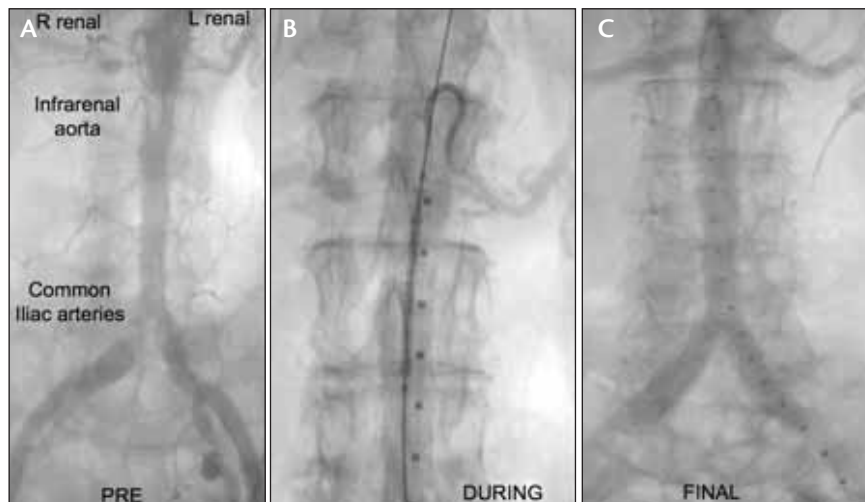


Figure 4. Preintervention evaluation of the renal artery, infrarenal aortic, and common iliac artery stenoses by angiography (A). Positioning of the aortic stent. A marker catheter has been placed from the contralateral femoral access site to indicate target lesion length and the location of the renal artery ostia (B). Final angiographic result after implanting aortic, bilateral renal artery, and bilateral common iliac artery bare-metal stents (C).

lesion and both renal arteries (Figure 5). Based on this information, the infrarenal aortic procedure was planned with use of a 10-mm-diameter balloon-expandable stent, with plans to postdilate with a 12-mm balloon. Both devices could be delivered via a 7-F sheath. The bilateral ostial iliac stenoses precluded the use of larger-size sheaths.

After securing left and right common femoral artery access, aortography was performed, and a 20-MHz IVUS imaging catheter was used over a 0.014-inch support wire to further assess the infrarenal aorta and the left common iliac artery stenosis (Figure 6). A 7- X 27-mm balloon-expandable stent was positioned across the left ostial common iliac artery lesion and a 7- X 37-mm balloon-expandable stent across the right ostial common iliac artery lesion; the sheaths were retracted to uncover the stents in an inverse V position. The stents were sequentially deployed at 14 atm inflation pressure, and then simultaneous kissing-balloon inflations were performed at 6 atm. A compliant 8- X 20-mm balloon was then used at 10 atm for 30 seconds to selectively expand the distal aspect of the right common iliac artery stent that was located at an area of poststenotic dilation distal to the ostium.

After removal of the balloon catheters, a marker 5-F pigtail catheter was advanced to the level of the renal arteries from the right side while the dilator was reinserted in the left side sheath and was subsequently advanced across the infrarenal aortic stenosis, which



Figure 5. Interrogation of the infrarenal aortic stenosis by CT scan. CT scanning shows diffuse, heavy calcification of the aortic wall, especially at the lesion site, and can accurately measure the distance from neighboring arterial ostia (superior mesenteric artery), as well as the target lesion length (A). The closest ostium to the largest lesion is the right renal (7.9 mm; 12.4 mm from the left renal artery). The stenosis is purely due to calcification and atherosclerosis without any aneurysmal contribution (14.7- X 15.6-mm outer wall dimensions, which is limited in visualization due to calcium-related shadowing) (B). The distal reference segment has circumferential calcification (as does the entire aorta); the outer-wall diameter is 13.5 mm (C).

was approximately 75% obstructive on angiography. The dilator was then exchanged for a 10- X 37-mm balloon-expandable stent, and the sheath was retracted to uncover the stent in position. Guiding angiography from the marker catheter was used to avoid stent deployment across the renal arteries (Figure 4), and then the diagnostic catheter was withdrawn. The stent was deployed with one inflation at 10 atm and was subsequently postdilated at 14 atm with a 10- X 12-mm balloon showing excellent angiographic and ultrasound results (Figures 4 and 6). The thoracic aorta-to-femoral pressure gradients were eliminated bilaterally.

Attention was subsequently given to the renal arteries. Using a no-touch technique with a 6-F, 55-cm internal mammary guiding catheter and a 190-cm, 0.014-inch wire, a 4- X 15-mm compliant monorail balloon was inflated at 14 atm across the 80% stenotic right renal artery lesion. A 5.5- X 15-mm balloon-expandable stent was subsequently deployed at 12 atm and flared. Using a similar technique after predilation, a 5- X 18-mm and then a 5- X 12-mm stent (both balloon-expandable) were serially deployed at 12 atm across the left renal artery lesion (90% stenotic, approximately 18–20 mm in length). Final flow and angiographic results were excellent.

The entire case was completed with limited iodinated contrast use (60 mL). Heparin (3,000 units intravenously) was used for anticoagulation, allowing the sheaths to be removed 2 hours after the procedure without complication. No decrease in hematocrit or increase in serum creatinine was observed postprocedure or at follow-up laboratory analysis.

CONCLUSION

Practice guidelines require a complete anatomical evaluation of the affected arterial territory, including

GORE® EXCLUDER® AAA Endoprosthesis

INDICATIONS FOR USE: Trunk-Ipsilateral Leg Endoprosthesis and Contralateral Leg Endoprosthesis Components. The GORE® EXCLUDER® AAA Endoprosthesis is intended to exclude the aneurysm from the blood circulation in patients diagnosed with infrarenal abdominal aortic aneurysm (AAA) disease and who have appropriate anatomy as described below: Adequate iliac / femoral access; Infrarenal aortic neck treatment diameter range of 19 – 29 mm and a minimum aortic neck length of 15 mm; Proximal aortic neck angulation ≤ 60°; Iliac artery treatment diameter range of 8 – 18.5 mm and iliac distal vessel seal zone length of at least 10 mm. **Aortic Extender Endoprosthesis and Iliac Extender Endoprosthesis Components.** The Aortic and Iliac Extender Endoprostheses are intended to be used after deployment of the GORE® EXCLUDER® AAA Endoprosthesis. These extensions are intended to be used when additional length and / or sealing for aneurysmal exclusion is desired. **CONTRAINDICATIONS:** The GORE® EXCLUDER® AAA Endoprosthesis is contraindicated in patients with known sensitivities or allergies to the device materials and patients with a systemic infection who may be at increased risk of endovascular graft infection. Refer to *Instructions for Use* at goremedical.com for a complete description of all warnings, precautions and adverse events. Rx Only



Products listed may not be available in all markets.
GORE®, EXCLUDER®, and designs are trademarks of W. L. Gore & Associates.
©2010 W. L. Gore & Associates, Inc. AP0830-EN1 DECEMBER 2010

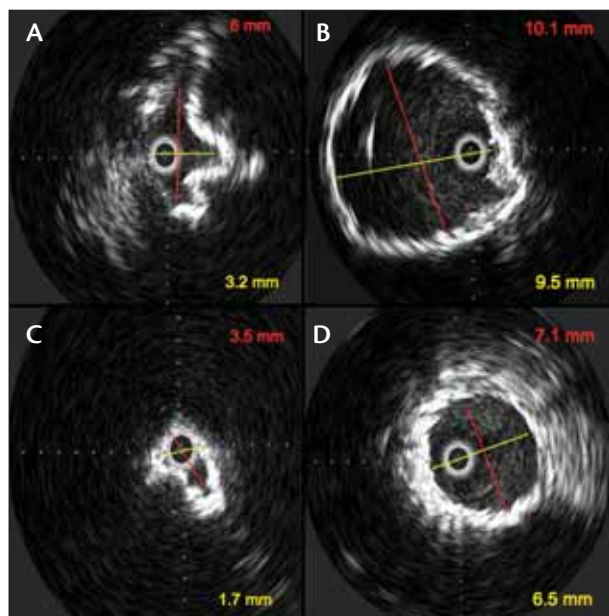


Figure 6. IVUS lumen dimensions of the infrarenal aortic stenosis before (A) (3.2 X 6 mm) and after (B) (9.5 X 10.1 mm) stenting. IVUS lumen dimensions of the left common iliac artery stenosis before (C) (1.7 X 3.5 mm) and after (D) (6.5 X 7.1 mm) intervention.

occlusive lesions as well as arterial inflow and outflow, before making decisions about revascularization. Although DSA remains the gold standard, noninvasive modalities are attractive alternate tools that have proven to be highly efficacious for the evaluation of PAD. Recognizing the potential advantages and disadvantages of these respective imaging modalities is an important aspect of contemporary clinical practice and endovascular revascularization. ■

José M. Wiley, MD, is Assistant Professor of Medicine at the Cardiovascular Institute, Mount Sinai Medical Center in New York. He has disclosed that he holds no financial interest in any product or manufacturer mentioned herein.

Prakash Krishnan, MD, is Assistant Professor of Medicine at the Cardiovascular Institute, Mount Sinai Medical Center, in New York. He has disclosed that he is a paid consultant to Abbott Vascular, Daiichi Sankyo, ev3 Inc., and Volcano Corporation.

Elias Sanidas, MD, is with the Antwerp Cardiovascular Institute Middelheim, Ziekenhuis Netwerk Antwerpen in Antwerp, Belgium. He has disclosed that he holds no financial interest in any product or manufacturer mentioned herein.

Jason C. Kovacic, MD, PhD, is an Associate at the Cardiovascular Institute, Mount Sinai Medical Center in

New York. He has disclosed that he holds no financial interest in any product or manufacturer mentioned herein.

George Dangas, MD, PhD, is Professor of Medicine at the Cardiovascular Institute, Mount Sinai Medical Center in New York. He has disclosed that he holds no financial interest in any product or manufacturer mentioned herein. Dr. Dangas may be reached at george.dangas@mountsinai.org.

1. Hiatt WR. Medical treatment of peripheral arterial disease and claudication. *N Engl J Med*. 2001;344:1608-1621.
2. Newman AB, Shemanski L, Manolio TA, et al. Ankle-arm index as a predictor of cardiovascular disease and mortality in the Cardiovascular Health Study. The Cardiovascular Health Study Group. *Arterioscler Thromb Vasc Biol*. 1999;19:538-545.
3. Dormandy J, Heeck L, Vig S. The fate of patients with critical leg ischemia. *Semin Vasc Surg*. 1999;12:142-147.
4. Kaatee R, Beek FJ, de Lange EE, et al. Renal artery stenosis: detection and quantification with spiral CTA versus optimized digital subtraction angiography. *Radiology*. 1997;205:121-127.
5. Sun Z. Diagnostic accuracy of multislice CTA in peripheral arterial disease. *J Vasc Interv Radiol*. 2006;17:1915-1921.
6. Ota H, Takase K, Igarashi K, et al. MDCT compared with digital subtraction angiography for assessment of lower extremity arterial occlusive disease: importance of reviewing cross-sectional images. *AJR Am J Roentgenol*. 2004;182:201-209.
7. Ouwendijk R, Kock MC, Visser K, et al. Interobserver agreement for the interpretation of contrast-enhanced 3D MRA and MDCTA in peripheral arterial disease. *AJR Am J Roentgenol*. 2005;185:1261-1267.
8. Martin ML, Tay KH, Flak B, et al. Multidetector CTA of the aortoiliac system and lower extremities: a prospective comparison with digital subtraction angiography. *AJR Am J Roentgenol*. 2003;180:1085-1091.
9. Rofsky NM, Johnson G, Adelman MA, et al. Peripheral vascular disease evaluated with reduced-dose gadolinium-enhanced MRA. *Radiology*. 1997;205:163-169.
10. Meaney JF, Ridgway JP, Chakraborty S, et al. Stepping-table gadolinium-enhanced digital subtraction MRA of the aorta and lower extremity arteries: preliminary experience. *Radiology*. 1999;211:59-67.
11. Poon E, Yucel EK, Pagan-Marín H, et al. Iliac artery stenosis measurements: comparison of two-dimensional time-of-flight and three-dimensional dynamic gadolinium-enhanced MRA. *AJR Am J Roentgenol*. 1997;169:1139-1144.
12. Wikstrom J, Holmberg A, Johansson L, et al. Gadolinium-enhanced magnetic resonance angiography, digital subtraction angiography and duplex of the iliac arteries compared with intra-arterial pressure gradient measurements. *Eur J Vasc Endovasc Surg*. 2000;19:516-523.
13. Visser K, Hunink MG. Peripheral arterial disease: gadolinium-enhanced MRA versus color-guided duplex US—a meta-analysis. *Radiology*. 2000;216:67-77.
14. Lakshminarayan R, Simpson JO, Ettles DF. Magnetic resonance angiography: current status in the planning and follow-up of endovascular treatment in lower-limb arterial disease. *Cardiovasc Interv Radiol*. 2009;32:397-405.
15. Maintz D, Tombach B, Juergens KU, et al. Revealing in-stent stenoses of the iliac arteries: comparison of multidetector CT with MRA and digital radiographic angiography in a Phantom model. *AJR Am J Roentgenol*. 2002;179:1319-1322.
16. Frayne R, Wehelié A, Yang Z, et al. MR Evaluation of Signal-Emitting Coatings. In: *Proceedings of the International Society for Magnetic Resonance in Medicine 7th Scientific Meeting and Exhibition*; Philadelphia, PA; 1999.
17. Rubin DL, Ratner AV, Young SW. Magnetic susceptibility effects and their application in the development of new ferromagnetic catheters for magnetic resonance imaging. *Invest Radiol*. 1990;25:1325-1332.
18. Bock M, Wacker FK. MR-guided intravascular interventions: techniques and applications. *J Magn Reson Imaging*. 2008;27:326-338.
19. Pentecost MJ, Criqui MH, Dorros G, et al. Guidelines for peripheral percutaneous transluminal angioplasty of the abdominal aorta and lower extremity vessels. A statement for health professionals from a special writing group of the Councils on Cardiovascular Radiology, Arteriosclerosis, Cardio-Thoracic and Vascular Surgery, Clinical Cardiology, and Epidemiology and Prevention, the American Heart Association. *Circulation*. 1994;89:511-531.